Chapter 4
Pareto Optimization of a Nonlinear Tuned Mass Damper to Control Vibrations in Hand Held Impact Machines

Seyed Milad Mousavi Bideleh and Viktor Berbyuk

Abstract Large amplitude vibrations from hand held impact machines might bring serious health problems for users in long term. Here, a vibration absorber which works based on the nonlinear tuned mass damper concept is applied to mitigate unpleasant vibrations in a hand held impact machine. A global sensitivity analysis is carried out using multiplicative dimensional reduction method to scrutinize the effects of different components on the hand held impact machine dynamics response and attenuate the number of input parameters for optimization. Based on the global sensitivity analysis results, the nonlinear tuned mass damper components are chosen as the design parameters subject to optimization. A multiobjective optimization problem is formulated and solved using genetic algorithm to reduce vibrations and total weight of the machine. The Pareto optimized solutions are robust against the exciting force amplitude and frequency. The global sensitivity analysis results revealed that it is possible to run the simulations with a constant exciting force amplitude and extend the obtained solutions for the case with a variable exciting force amplitude while the same order of accuracy in the results can be observed. This significantly reduced the computational burden of the optimization. Closed form expressions for the optimal values of the tuned mass damper parameters as well as system response in terms of the auxiliary mass are developed by using the nonlinear least squares method. The results revealed that the proposed technique can significantly suppress the vibrations induced by the hand held impact machine. This makes it possible for users to operate the machine for a longer time period with lower health risks.

Keywords Nonlinear tuned mass damper · Hand held impact machine · Weight-vibration Pareto optimization · Global sensitivity analysis · M-DRM

4.1 Introduction

Efficiency, simplicity, and low maintenance cost are some of the most important features of tuned mass damper (TMD) technology which make it possible to employ this technique in a variety of engineering applications. Yang et al. [1] designed a two degrees of freedom (DOFs) TMD to damp the dominant mode of the workpiece/fixture assembly in milling process. The experimental results revealed around 80 percent reduction in the amplitude of the dominant mode using the two proposed techniques which was more efficient in comparison with to a single DOF and two single DOF TMDs with equal mass. Li and Tang [2] integrated a particle damping mechanism into a TMD configuration. Such a combination significantly magnified the energy dissipation capacity of the TMD especially when the host structure vibrates with low amplitudes. The proposed technique could also be used in harsh conditions such as high temperatures where ordinary fluid dampers might fail. Dinh and Basu [3] investigated the application of multiple TMDs in mitigating nacelle and spar vibrations of floating offshore wind turbines. The performance of the proposed multiple TMDs has been tested under different loading conditions. The results also showed that vibration reduction is not much improved by using more than two TMDs.

Optimization of TMD properties has been considered by many researchers, see e.g. [4–8]. Genetic algorithm (GA) is one of the most powerful tools in multiobjective design optimization of mechanical and structural systems, see e.g. [9–11]. Ok et al. [12] utilized a fast elitist non-dominated sorted GA to solve the multiobjective optimization problem of finding the optimal properties of a bi-tuned mass damper. The multiobjective optimization problem has been considered for different

S. M. Mousavi Bideleh
Multibody Dynamics, VETEC AB, Mölndal, Sweden
e-mail: milad.mousavi@vetec.se

V. Berbyuk (✉)
Department of Mechanics and Maritime Sciences, Chalmers University of Technology, Göteborg, Sweden
e-mail: viktor.berbyuk@chalmers.se

G. Kerschen (ed.), *Nonlinear Dynamics, Volume 1*, Conference Proceedings of the Society for Experimental Mechanics Series, https://doi.org/10.1007/978-3-319-74280-9_4

mass ratios to account for the respective effects on the control performance. By using the Pareto optimal solutions of each case and a nonlinear curve fitting technique, closed-form expressions for optimal tuning frequencies and damping ratios of bi-tuned mass dampers have been derived. Mohtat and Dehghan-Niri [13] utilized GA for robust design of TMD systems with application in multi-story buildings. The overall dynamics of the system has been modeled using a linear fractional transformation framework which isolated the TMD as a feedback controller. This approach made it possible to apply the active structural control concepts in passive design of TMDs. Greco et al. [14] employed GA to solve the multiobjective optimization design problem of a TMD to control the vibrations in buildings under low-moderate earthquakes. Cost and efficiency of the TMD device have been considered as two objective functions for optimization. The simulations showed that best TMD performance is achieved when the frequency of the main system is around the resonance region. Furthermore, the TMD yield higher performance for structures with a low damping. Detroux et al. [15] considered the performance, robustness, and sensitivity analysis of a nonlinear tuned vibration absorber. The effects of different design parameters and force amplitudes on the performance and operation region of the nonlinear tuned vibration absorber have been analyzed.

Multidisciplinary and multiobjective design optimization is basically a time costly procedure. Number of input design parameters can significantly affect the computational efforts for optimization. Therefore, as a preliminary stage in multidisciplinary design optimization of mechanical systems, it is necessary to carry out sensitivity analysis of the system response with respect to different design parameters. This makes it possible to narrow down the number of inputs for optimization and improve the computational efficiency of the algorithm. Zhang and Pandey [16] proposed an efficient algorithm for global sensitivity analysis (GSA) which worked based on a multiplicative dimensional reduction method (M-DRM). In the M-DRM, a given deterministic function is approximated by low dimensional functions which significantly simplifies high dimensional integrals required to calculate the sensitivity indices. The method has been applied to some simple mechanical and mathematical examples and the results showed excellent agreement with those associated with the Monte Carlo simulation. Mousavi Bideleh and Berbyuk employed this approach to study the effects of elastic suspension components of a high speed train on the overall performance of the vehicle, see e.g. [17, 18]. The results revealed that the proposed method is capable to accomplish the GSA for complex nonlinear systems with many DOFs in a computationally efficient manner.

Early it was shown that incorporation of a TMD into a hand held impact machine (HHIM) can significantly reduce the vibrations [19]. The present paper is a continuation of the work done in [19] and is focused on Pareto optimization of the TMD parameters in HHIMs. By using the M-DRM, the GSA is carried out for a 3 DOFs mechanical system which represents the HHIM with TMD. Then, a bi-objective optimization problem is considered to simultaneously reduce the weight and vibrations in the machine on a wide operation range of frequency and amplitude. The obtained results are analyzed and presented as Pareto front and Pareto set. The nonlinear least squares method is used to derive analytical expressions for relationships between the mass of the nonlinear TMD and optimized stiffness, gap, and preload values.

4.2 Engineering and Mathematical Models

The pneumatic HHIM comprises of a handle housing, an air inlet valve, a main body, a piston, an air outlet, a cylinder, a chisel, an auxiliary mass as well as several stiffness and damping components. The engineering model of the considered HHIM is depicted in Fig. 4.1a and is described more in detail in [19]. A 3 DOFs mechanical system is chosen to represent the HHIM with TMD. The sketch of the HHIM as a 3 DOFs system is shown in Fig. 4.1b. Parameters k_a, a, and F_0 represent the TMD stiffness, the half gap length, and the spring preload, respectively. Rest of the notations used to describe the HHIM model and respective values are given in Table 4.1. Vector $\mathbf{x}(t) = [x_1, x_2, x_3]^T$ is chosen as the vector of coordinates of the vibrating system as depicted in Fig. 4.1b.

The equations of motion for the 3 DOFs system shown in Fig. 4.1b are given [19]:

$$m_m\ddot{x}_1 + (c_m + c_h)\dot{x}_1 - c_h\dot{x}_3 + (k_m + k_h)x_1 - k_h x_3 = F_e(t) + F_k(\mathbf{x}) + F_c(\mathbf{x}, \dot{\mathbf{x}}) - m_m g \tag{4.1}$$

$$m_a\ddot{x}_2 = -F_k(\mathbf{x}) - F_c(\mathbf{x}, \dot{\mathbf{x}}) - m_a g \tag{4.2}$$

$$m_h\ddot{x}_3 - c_h\dot{x}_1 + (c_h + c_p)\dot{x}_3 - k_h x_1 + (k_h + k_p)x_3 = -m_h g \tag{4.3}$$

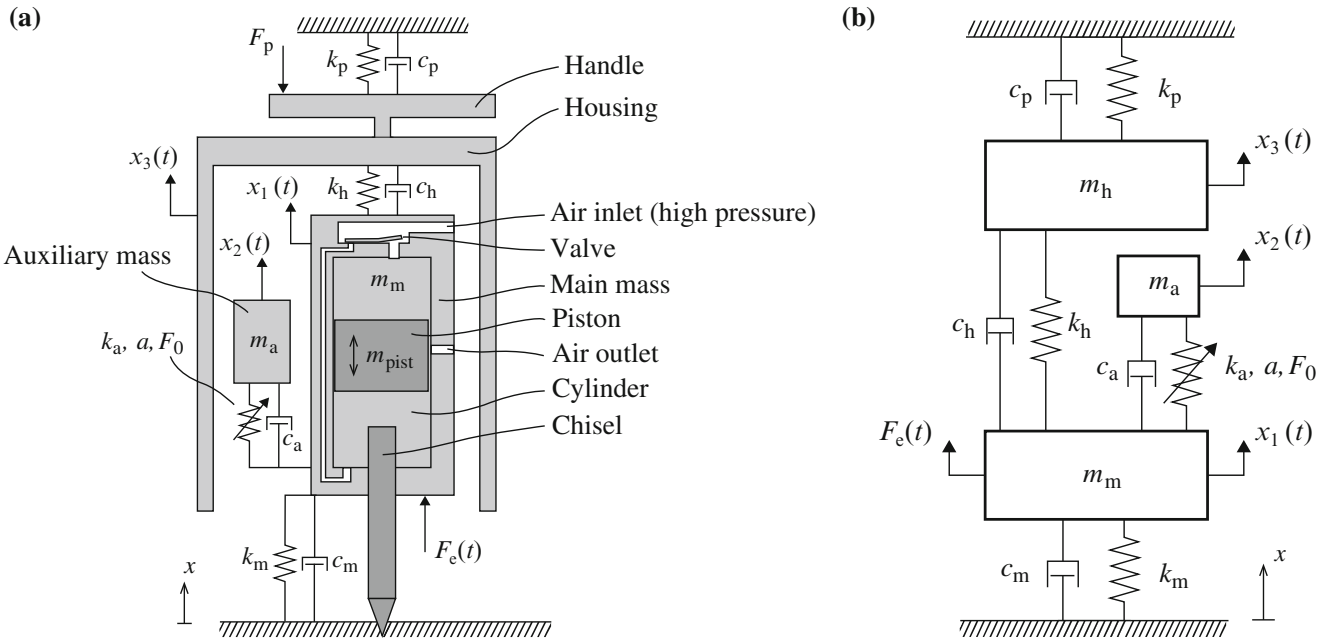

Fig. 4.1 Structure of the HHIM: (**a**) Engineering model; (**b**) 3 DOFs equivalent model [19]

Table 4.1 Structural parameters of the HHIM

Parameter	Nominal value	Description
m_m [kg]	2.7	The main body mass
m_a [kg]	1	The auxiliary mass
m_h [kg]	3.1	The housing mass
k_m [kN/m]	0.5	The stiffness between main mass and ground
k_h [kN/m]	14	The stiffness between main mass and housing
k_p [kN/m]	1	The hand arm stiffness
c_m [Ns/m]	100	The damping between main mass and ground
c_a [Ns/m]	1	The damping of the TMD
c_h [Ns/m]	20	The damping between main mass and housing
c_p [Ns/m]	60	The hand arm damping

In Eqs. (4.1, 4.2 and 4.3), functions $F_k(\mathbf{x})$ and $F_c(\mathbf{x}, \dot{\mathbf{x}})$ are stiffness and damping forces exerted by the TMD and function $F_e(t)$ is the periodic external excitation force acting on the HHIM.

In case when the functions $F_k(\mathbf{x})$ and $F_c(\mathbf{x}, \dot{\mathbf{x}})$ are given by the following expression.

$$F_k(\mathbf{x}) = k_a(x_2 - x_1), \tag{4.4}$$

$$F_c(\mathbf{x}, \dot{\mathbf{x}}) = c_a(\dot{x}_2 - \dot{x}_1), \tag{4.5}$$

the Eqs. (4.1, 4.2 and 4.3) with expressions (4.4 and 4.5) and the following initial states:

$$\begin{cases} \mathbf{x}(t_0) = \mathbf{x}_0 \\ \dot{\mathbf{x}}(t_0) = \dot{\mathbf{x}}_0 \end{cases}, \tag{4.6}$$

constitute the mathematical model of the HHIM equipped with linear TMD (L-TMD).

Alternatively, it is also assumed that the stiffness force exerting by the TMD is determined by the following nonlinear expression [19]:

$$F_k(\mathbf{x}) = \begin{cases} F_0 + k_a(x_2 - x_1 - a) & \text{if } x_2 - x_1 > a \\ -F_0 - k_a(-x_2 + x_1 - a) & \text{if } x_2 - x_1 < -a \\ 0 & \text{else} \end{cases} \tag{4.7}$$

The Eqs. (4.1, 4.2 and 4.3), expressions (4.5 and 4.7) together with the initial states (4.6) constitute the mathematical model of the HHIM with nonlinear TMD (N-TMD).

Some verification and experimental validation results of the presented mathematical models can be found in [19].

4.3 Objective Functions and Design Parameters

In what follows several problems on sensitivity analysis and optimization of the HHIM are considered within the L-TMD and N-TMD models.

To study the design of the HHIM as well as its performance several characteristics and objective functions are used. For both L-TMD and N-TMD models the following objective functions given by Eqs. (4.8 and 4.9) are introduced to measure the vibrations induced to the user by the HHIM

$$\Gamma_{\text{Dis}}(f) = \max_f \{\text{RMS}(x_3(t))\}, \tag{4.8}$$

$$\Gamma_{\text{Vol}} = \int_{F_{\text{eref}}^{\min}}^{F_{\text{eref}}^{\max}} \int_{f_{\min}}^{f_{\max}} \text{RMS}(x_3(t))\ df\ dF_{\text{eref}}, \tag{4.9}$$

where $\text{RMS}(x_3(t)) = \sqrt{\frac{1}{t_f - t_0}\int_{t_0}^{t_f}(x_3(t))^2 dt}$.

Variables $f \epsilon [f_{\min}, f_{\max}\ ]$ and $F_{\text{eref}} \epsilon \left[F_{\text{eref}}^{\min}, F_{\text{eref}}^{\max}\right]$ are the frequency and the reference value of amplitude of the harmonic external excitation force, respectively.

Objective function Γ_{Disp} indicates the maximum RMS value of $x_3(t)$ amplitude within the frequency range.

Objective function Γ_{Vol} is the volume below the surface surrounded by frequency, exciting force amplitude and RMS of the vibration. Indeed, in this case the aim is to minimize the RMS value of vibrations on a set of desired frequency and force amplitude ranges.

For the GSA and optimization of the HHIM different vectors of varying parameters are considered. Furthermore, the sensitivity of the natural frequencies and damping ratios will be study with respect to the vector of all structural parameters of the 3 DOFs HHIM with the L-TMD. The vector of input design parameters ($\mathbf{d_s}$) for GSA is given by Eq. (4.10).

$$\mathbf{d}_{\text{s}} = \left[m_{\text{m}}, m_{\text{a}}, m_{\text{h}}, k_{\text{m}}, k_{\text{a}}, k_{\text{h}}, k_{\text{p}}, c_{\text{m}}, c_{\text{a}}, c_{\text{h}}, c_{\text{p}}\right]^{\text{T}}. \tag{4.10}$$

The following vector of varying parameters will be used to study the sensitivity of the machine vibration level in case of utilization of the L-TMD in the HHIM:

$$\mathbf{d}_{\text{l}} = \left[m_{\text{a}}, k_{\text{m}}, k_{\text{a}}, k_{\text{h}}, k_{\text{p}}, c_{\text{m}}, c_{\text{a}}, c_{\text{h}}, F_{\text{eref}}\right]^{\text{T}}. \tag{4.11}$$

The GSA of vibration level of the HHIM equipped with the nonlinear TMD will be considered with respect to the following vector of varying parameters:

$$\mathbf{d}_{\text{n}} = \left[m_{\text{a}}, k_{\text{m}}, k_{\text{a}}, k_{\text{h}}, k_{\text{p}}, c_{\text{m}}, c_{\text{a}}, c_{\text{h}}, a, F_0, F_{\text{eref}}\right]^{\text{T}}. \tag{4.12}$$

In the case of multiobjective optimization problem, the vector of input design parameters for the HHIM with the linear TMD is considered as:

$$\mathbf{d}_{\text{pl}} = [m_{\text{a}}, k_{\text{a}}]^{\text{T}}. \tag{4.13}$$

For the Pareto optimization of the HHIM with the nonlinear TMD, the vector of varying parameters is chosen as:

$$\mathbf{d}_{\mathrm{pn}} = [m_{\mathrm{a}}, k_{\mathrm{a}}, a, F_0]^{\mathrm{T}}. \tag{4.14}$$

4.4 Global Sensitivity Analysis

Sensitivity analysis can be carried out either locally or globally. Local sensitivity is often measured by taking derivative of an objective function with respect to a particular design parameter around a fixed point in space. Therefore, the interaction of different design variables on an objective function is not properly reflected and the sensitivity highly depends on the chosen fixed point.

GSA is capable to thoroughly scan the domain of the input design variables and take into account the simultaneous effects of different design parameters on a particular objective function. However, large numbers of sample data required to achieve a satisfactory level of accuracy as well as evaluation of high dimensional integrals are some of the most important drawbacks within ordinary GSA methods.

Several approaches are developed to improve the computational efficiency of the GSA algorithms. Analysis of variance (ANOVA) decomposition, also known as high dimensional model representation (HDMR), decomposes a function into a set of sub functions and is a powerful tool in GSA, see, e.g., [20–22]. An efficient approximation of HDMR is cut-HDMR in which a particular function is decomposed around a set of points, planes, or hyper planes. Each objective function (Γ) can be expressed as functions of a set of n independent random variables $\mathbf{X} = [x_1, x_2, \ldots, x_n]^{\mathrm{T}}$, through the respective functional relationship $\Gamma = \mathcal{F}(\mathbf{X})$, with $\mathbf{X}$ as the vector of design parameters. Based on the cut-HDMR concept, function $\mathcal{F}(\mathbf{X})$ is decomposed around the vector $\mathbf{c} = [c_1, \ldots, c_n]^{\mathrm{T}}$. This vector is known as cut center and contains nominal values of the design parameters. Finally, $\mathcal{F}(x_i, \mathbf{c}_{-i})$ denotes the function value for the case that all inputs except x_i, are fixed at their respective cut point coordinates.

Zhang and Pandey [16] used the cut-HDMR approach and proposed a M-DRM which simplifies the calculation of high dimensional integrals and yields the closed-form formulation for the global sensitivity index of an objective function with respect to the ith design parameter x_i:

$$S_i^{\mathrm{T}} \approx \frac{1 - \alpha_i^2/\beta_i}{1 - \left(\prod_{k=1}^{n} \alpha_k^2/\beta_k\right)}, \tag{4.15}$$

here, S_i^{T} is the total sensitivity index.

Variables α_k and β_k are calculated using Gaussian quadrature integration method:

$$\begin{cases} \alpha_k \approx \sum_{l=1}^{N} w_{kl} \mathcal{F}\left(x_{kl}, \mathbf{c}_{-kl}\right) \\ \beta_k \approx \sum_{l=1}^{N} w_{kl} [\mathcal{F}\left(x_{kl}, \mathbf{c}_{-kl}\right)]^2 \end{cases}, \tag{4.16}$$

here, N is the total number of integration points, x_{kl} and w_{kl} are the lth Gaussian integration abscissa and the corresponding weight, respectively. Note that α_i and β_i are also evaluated using Eqs. (4.16). Indeed, the numerator in Eq. (4.15) considers the effects of the ith design parameter (x_i), while the denominator takes into account the product of the effects of all the design parameters.

The total number of function evaluations required to calculate the sensitivity indices using this method is only $n \times N$. This approach is already verified against Monte Carlo simulation through some simple mathematical and mechanical examples [16]. The efficiency of this method for GSA of multibody systems is also shown in [17, 18]. More details on GSA and M-DRM approaches can be found in [16, 23, 24].

4.5 Multidisciplinary Design Optimization

The target of this study is to minimize vibrations and the weight of the HHIM. The multiobjective design optimization problem is then formulated as follows:

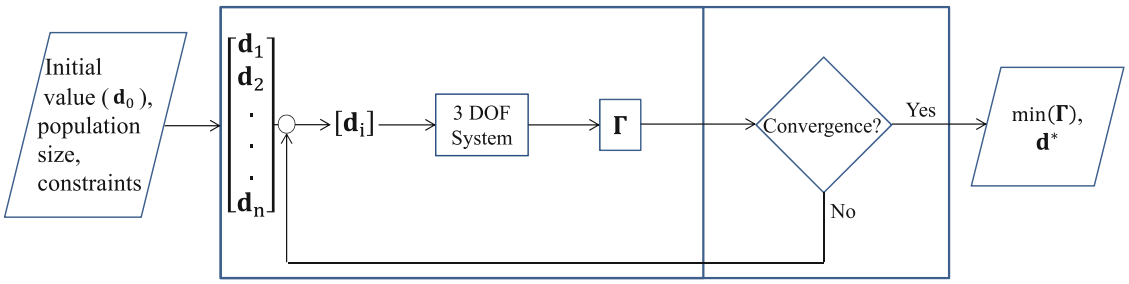

Fig. 4.2 Optimization flowchart

For the given HHIM model shown in Fig. 4.1 and prescribed structural parameters, it is required to determine the optimized vector of the design parameters ($\mathbf{d}^*$) such that the variational Eq. (4.17) is satisfied

$$\mathbf{\Gamma}\left(\mathbf{d}^*\right) = \min_{\mathbf{d}\in\Omega} \mathbf{\Gamma}\left(\mathbf{d}\right) \tag{4.17}$$

subject to differential constraints Eqs. (4.1, 4.2 and 4.3) and feasible initial states Eq. (4.6). Here, $\mathbf{\Gamma}$ is the vector of objective functions, and Ω is the domain of the input design variables ($\mathbf{d}$). The solution of Eq. (4.17) yields Pareto optimized vector of the design parameters ($\mathbf{d}^*$).

4.5.1 Optimization Algorithm

To solve the formulated problem, an evolutionary multiobjective optimization algorithm which works based on GA is implemented in MATLAB. For the initial values of the design parameters ($\mathbf{d_0}$), and based on the prescribed settings, the GA generates the vector of sample design parameters ($\mathbf{d_i}$). The dynamics response of the system and objective functions are evaluated based on the mathematical model of the HHIM. This procedure is continued until convergence or the maximum number of iterations is achieved. The flowchart of the multiobjective optimization procedure is depicted in Fig. 4.2.

4.5.2 Operational Scenarios

Two sets of operational scenarios (OS) are considered for the analysis:

1. Simulations run with a fixed reference force amplitude ($F_{\mathrm{e_{ref}}}$) on a desired frequency range between 23–32 Hz. The vector of objective functions in this case is $\mathbf{\Gamma_{OS1}} = [\Gamma_{\mathrm{Disp}}/\ \Gamma^0_{\mathrm{Disp}}\ m_{\mathrm{a}}/m_a^0]^{\mathrm{T}}$. Here, Γ_{Disp} is determined by Eq. (4.8), the superscript "0" denotes the objective function value corresponding to the initial guess design parameters.
2. Simulations run with a variable reference force amplitude $0.8F_{\mathrm{e_{ref}}} \leq F_{\mathrm{e_{ref}}} \leq 1.2F_{\mathrm{e_{ref}}}$ on the desired frequency range between 23 and 32 Hz. The vector of objective functions for the second OS is defined as $\mathbf{\Gamma_{OS2}} = [\Gamma_{\mathrm{Vol}}/\ \Gamma^0_{\mathrm{Vol}}\ m_{\mathrm{a}}/m_a^0]^{\mathrm{T}}$, where Γ_{Vol} is determined by Eq. (4.9).

4.6 Results

The GSA and multiobjective optimization results are presented in this section. The results of linear and nonlinear TMD systems are also analyzed and compared.

4.6.1 GSA Results

In all sections of this paper, a lognormal distribution of the input design parameters with $N = 20$ Gaussian quadrature abscissas for numerical integrations is considered to carry out the GSA. The mean values of the design parameters are given in Table 4.1. The coefficient of variation (COV) used in different GSA problems is chosen in a way that the respective variation is remained within the admissible ranges for each particular design parameter, see Table 4.2.

4.6.1.1 Linear System

The total global sensitivity indices of the natural frequencies ($S^{\mathrm{T}}_{\omega_{\mathrm{n}_i}}$) and corresponding damping ratios ($S^{\mathrm{T}}_{\xi_{\mathrm{n}_i}}$) with $i = 1, 2, 3$ as function of the design parameters are shown in Fig. 4.3 for the linear 3 DOFs system. Each color box represents the respective sensitivity index. The higher sensitivity index reflects the higher effect of a particular design parameter on an objective function.

It should be noted that all the six objective functions (natural frequencies and damping ratios) are simultaneously evaluated and the number of function evaluations to achieve the GSA results shown in Fig. 4.3 is merely $N \times n_{\mathrm{d}} = 20 \times 11 = 220$.

As it follows from Fig. 4.3 the natural frequency of the first vibration mode (ω_{n_1}) is mostly sensitive with respect to the hand-arm and chisel stiffnesses (k_{m} and k_{p}). The damping ratio (ξ_1) at this vibration mode is mainly affected by the chisel mass m_{m} and linear TMD parameters (i.e. k_{a} and m_{a}). Therefore, the linear TMD mainly contributes in damping out the vibrations corresponding to the first vibration mode. The housing stiffness (k_{h}) together with the housing mass (m_{h}) and

Table 4.2 COVs used for GSA

m_{m}	m_{a}	m_{h}	k_{m}	k_{a}	k_{h}	k_{p}	c_{m}	c_{a}	c_{h}	c_{p}	a	F_0	F_{eref}
0.10	0.11	0.10	0.30	0.15	0.15	0.18	0.11	0.38	0.25	0.10	0.13	0.15	0.12

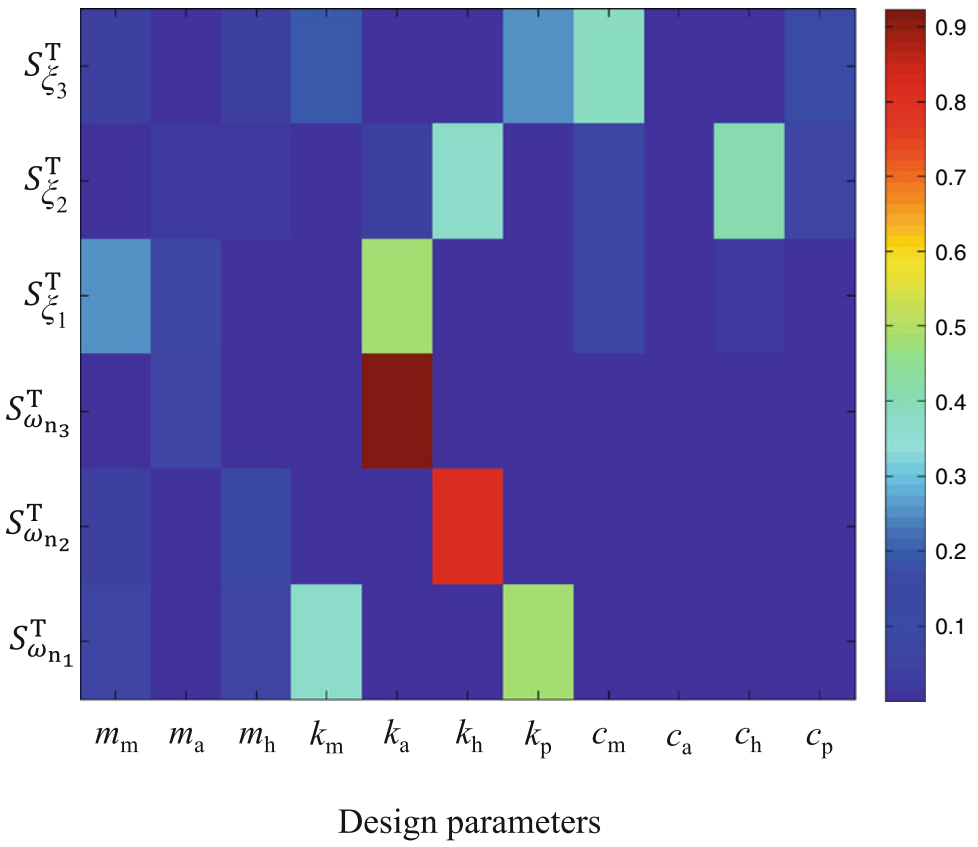

Fig. 4.3 Sensitivity indices of natural frequencies and damping ratios of the linear 3DOF system

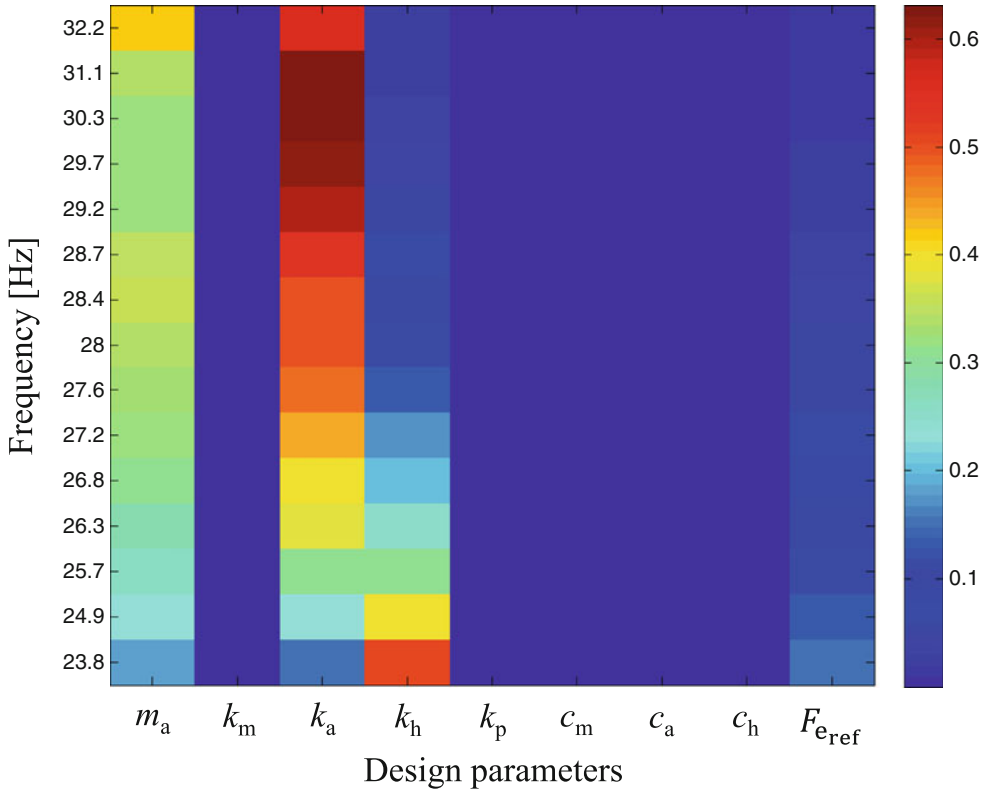

Fig. 4.4 Sensitivity of Γ_{Disp} at different exciting frequencies with respect to design parameters for the linear TMD

housing damping (c_h) are the most important parameters that can affect the second natural frequency (ω_{n_2}) and damping ratio (ξ_2), respectively. Finally, the third natural frequency of the system highly depends on the linear TMD parameters (i.e. k_a and m_a).

In order to use the 3 DOFs system given by Eqs. (4.1, 4.2, 4.3, 4.4, 4.5, 4.6 and 4.7) as a reference model for multidisciplinary design optimization of a HHIM, some practical design constraints have to be addressed. In this regard, the chisel mass (m_m), the housing mass (m_h), and the hand-arm damping (c_p) are considered constant during the subsequent sections inasmuch as those parameters are either fixed and/or already determined by the HHIM manufacturers. Therefore, the focus is on GSA and multiobjective optimization of the rest of the parameters.

The total global sensitivity indices of the maximum RMS value of x_3, ($S^{\text{T}}_{\Gamma_{\text{Disp}}}$), at different exciting frequencies (23.8 Hz $\leq f \leq$ 32.2 Hz) with respect to the design parameters are plotted in Fig. 4.4 for the linear TMD. It can be seen that the TMD parameters (i.e. m_a and k_a), the stiffness between the main mass and housing (k_h), and the reference force amplitude ($F_{e_{ref}}$) are the most important variables that can influence Γ_{Disp} in the desired frequency range.

The auxiliary mass m_a has almost a consistent effect on machine vibration estimated by the objective function given by Eq. (4.8). In lower frequencies the TMD parameters (m_a and k_a) have more or less similar effects on the vibration level. However, as long as the exciting frequency increases, the effects of the stiffness k_a becomes dominant. The sensitivity indices of parameters k_h and $F_{e_{ref}}$ reflect an opposite behavior. In other words, k_h and $F_{e_{ref}}$ have a more important influence on the machine vibration at lower exciting frequencies and by increasing the frequency, the respective effects become less important.

The values of total sensitivity index of the objective function Γ_{Vol} that estimates the machine vibration by using Eq. (4.9) on the prescribed range of the exciting force amplitude ($0.8F_{e_{ref}} \leq F_{e_{ref}} \leq 1.2F_{e_{ref}}$) and frequency (23.8 Hz $\leq f \leq$ 32.2 Hz) are presented in Fig. 4.5. It can be seen that the volume below the exciting force amplitude ($F_{e_{ref}}$), frequency (f), and the maximum RMS value of x_3 is mostly sensitive with respect to the linear TMD parameters (i.e. auxiliary mass (m_a) and stiffness (k_a)) and the housing stiffness (k_h).

The GSA results of Γ_{Disp} and Γ_{Vol} showed that the linear TMD parameters have the most important influence on the machine vibrations. Therefore, the auxiliary mass (m_a) and stiffness (k_a) are considered as the design parameters for multiobjective optimization of the linear TMD. Indeed, the auxiliary mass (m_a) is simultaneously considered as one of the design parameters and objective functions.

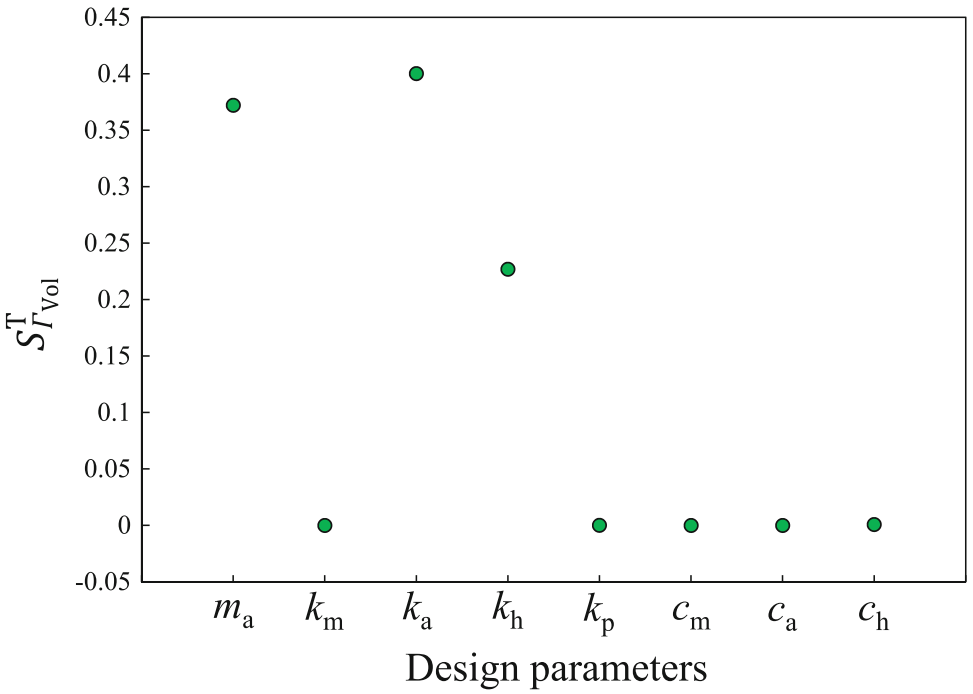

Fig. 4.5 Sensitivity of $\boldsymbol{\Gamma}_{\mathbf{Vol}}$ with respect to the design parameters for the linear TMD

4.6.1.2 Nonlinear System

The values of the total global sensitivity index of the maximum RMS value of x_3 ($S^{T}_{\Gamma_{Disp}}$) at different exciting frequencies are presented in Fig. 4.6 for the nonlinear TMD.

It can be seen that the objective function Γ_{Disp} is mostly influenced by the nonlinear TMD parameters (i.e. auxiliary mass m_a, auxiliary stiffness k_a, gap a, and preload F_0). At lower exciting frequencies, all the nonlinear TMD parameters have to some extent similar impact on machine vibration estimated by using the objective function Γ_{Disp}. However, as long as the exciting frequency increases, the effects of the auxiliary mass (m_a) and stiffness (k_a) become dominant. From this point of view, m_a and k_a exhibit the same behavior for linear and nonlinear TMDs, see Figs. 4.4 and 4.6. In contrast, the effects of gap (a) and preload (F_0) decay as long as the exciting frequency increases.

The GSA results shown in Fig. 4.6 provide informative data regarding the influence of different design parameters on Γ_{Disp} at different exciting force frequencies which can be beneficial in formulating the multiobjective optimization problem. As an example, assume that only two design parameters can be considered for optimization due to the practical and/or cost constraints. Therefore, if the operational frequency of the HHIM is around 26 Hz, it is recommended to choose the auxiliary mass (m_a) and the gap (a) as the design parameters for optimization. While, if the operational frequency of the HHIM is around 29 Hz, it is recommended to choose the auxiliary mass and stiffness (m_a and k_a) as the design parameters, see Fig. 4.6.

The exciting force amplitude ($F_{e_{ref}}$) has a more important influence on Γ_{Disp} at lower exciting frequencies rather than higher frequencies. This behavior has also been observed in the linear TMD case, see Fig. 4.4. The GSA results shown in Figs. 4.4 and 4.6 revealed that the exciting force amplitude ($F_{e_{ref}}$) cannot significantly influence the system response (Γ_{Disp}) in either linear or nonlinear TMDs (especially for higher exciting frequencies). This might make it possible to run the multiobjective optimization with a constant exciting force amplitude ($F_{e_{ref}}$) and apply the obtained Pareto optimized solutions for cases with a variable $F_{e_{ref}}$. In other words, the GSA results reveal that it is possible to carry out multiobjective optimization for $\boldsymbol{\Gamma}_{\mathbf{OS1}}$ and expect to achieve near optimal system behavior once utilizing the results obtained as the solutions to the multiobjective optimization problem with respect to $\boldsymbol{\Gamma}_{\mathbf{OS2}}$. This can significantly reduce the computational burden of optimization. Therefore, the GSA results can actively contribute in deciding the desired operational scenario for running the multiobjective optimization problems. The Pareto optimized solutions of the optimization problems with respect to $\boldsymbol{\Gamma}_{\mathbf{OS1}}$ and $\boldsymbol{\Gamma}_{\mathbf{OS2}}$ are compared and analyzed in Sect. 4.6.2 to better clarify the role of GSA on formulation of the multiobjective optimization problem.

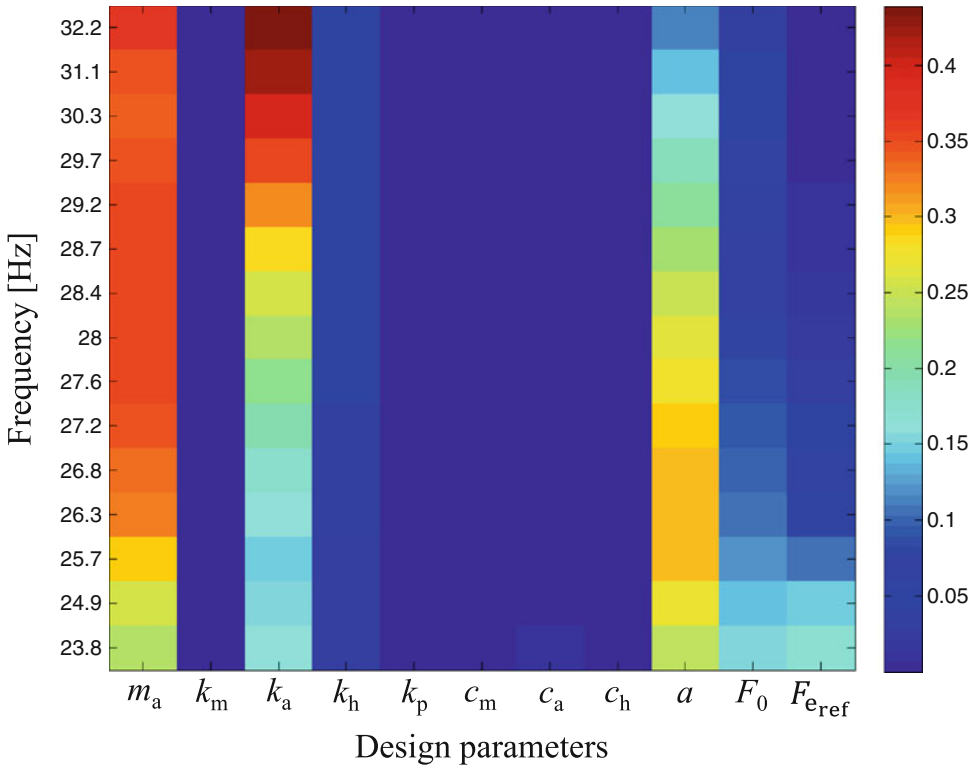

Fig. 4.6 Sensitivity of Max RMS of x_3 at different frequencies with respect to the design parameters for the nonlinear TMD

The values of the total sensitivity index of the objective function Γ_{Vol} for the nonlinear TMD in case that both the exciting force amplitude ($F_{e_{ref}}$) and frequency (f) are varying (i.e. OS2) are presented in Fig. 4.7.

It can be seen that the nonlinear TMD parameters i.e. the auxiliary mass (m_a) and stiffness (k_a), gap (a), and preload (F_0) have the most important effect on machine vibration estimated by the objective function Γ_{Vol}.

One interesting note is that although the housing stiffness (k_h) exhibit a remarkable influence on Γ_{Disp} or Γ_{Vol} for the linear TMD (Figs. 4.4 and 4.5), similar behavior is not observed for the nonlinear TMD. In this case, housing stiffness k_h does not reflect a remarkable influence on either Γ_{Disp} or Γ_{Vol} (see, Figs. 4.6 and 4.7). This shows one of the limitations of the linear TMD system.

Based on the GSA results, the TMD parameters (m_a and k_a for the linear case and m_a, k_a, a, and F_0 for the nonlinear case) are considered as the design parameters for optimization problems with respect to $\mathbf{\Gamma_{OS1}}$ and $\mathbf{\Gamma_{OS2}}$. The Pareto optimized solutions are discussed in the next section.

4.6.2 Multiobjective Optimization Results

The GA is utilized to carry out the multiobjective optimization. Population size and number of generations are set to 50 which give the number of maximum iterations equal to 2551. Based on the chosen GA settings, the Pareto set and Pareto front include 25 Pareto optimal solutions to the multiobjective optimization problem. The Pareto sets associated with OS1 and OS2 are shown in Fig. 4.8 for the linear TMD.

The Pareto fronts for the linear and nonlinear TMDs associated with OS1 and OS2 are plotted in Fig. 4.9. It should be noted that there is a mapping between the linear TMD results shown in Figs. 4.8 and 4.9. Indeed, each point in the Pareto set (Fig. 4.8) corresponds to a point in the Pareto front given in Fig. 4.9.

It can be seen that vibration absorption capacity of the linear TMD is improved by increasing the auxiliary mass (m_a) and stiffness (k_a) in both operational scenarios (OS1 and OS2). In other words, the maximum RMS of x_3 (Γ_{Disp}) as well as the volume between frequency (f), reference force amplitude ($F_{e_{ref}}$), and maximum RMS of x_3 measured as Γ_{Vol} are reduced by choosing some stiffer k_a and a more massive m_a. However, increasing m_a deteriorates the other objective function i.e. the total weight of the HHIM.

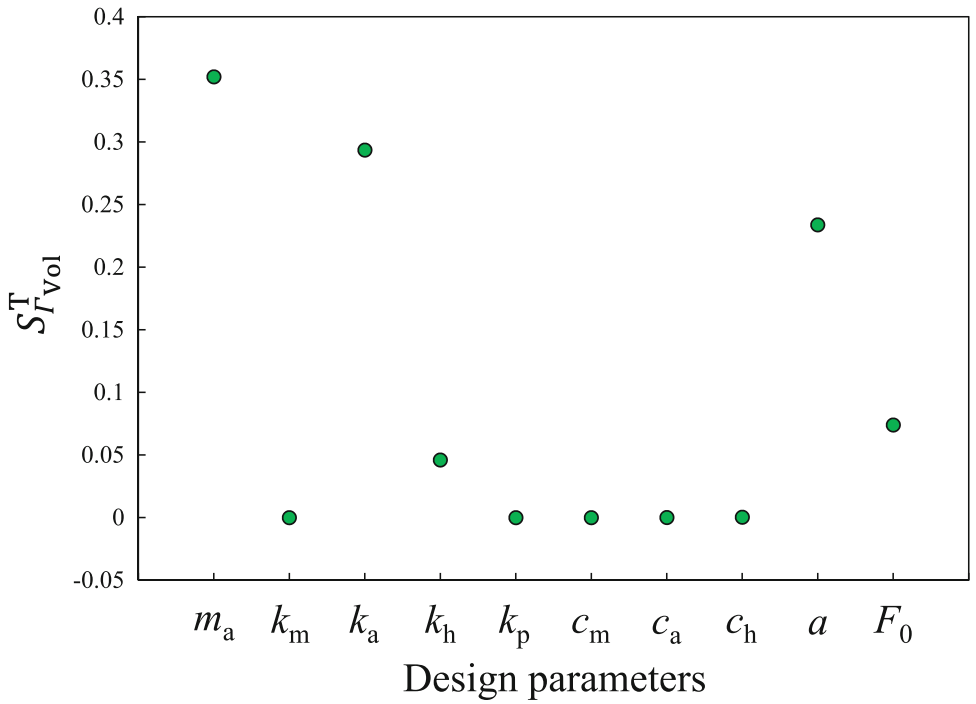

Fig. 4.7 Sensitivity of $\boldsymbol{\Gamma}_{\mathbf{Vol}}$ with respect to the design parameters for the nonlinear TMD

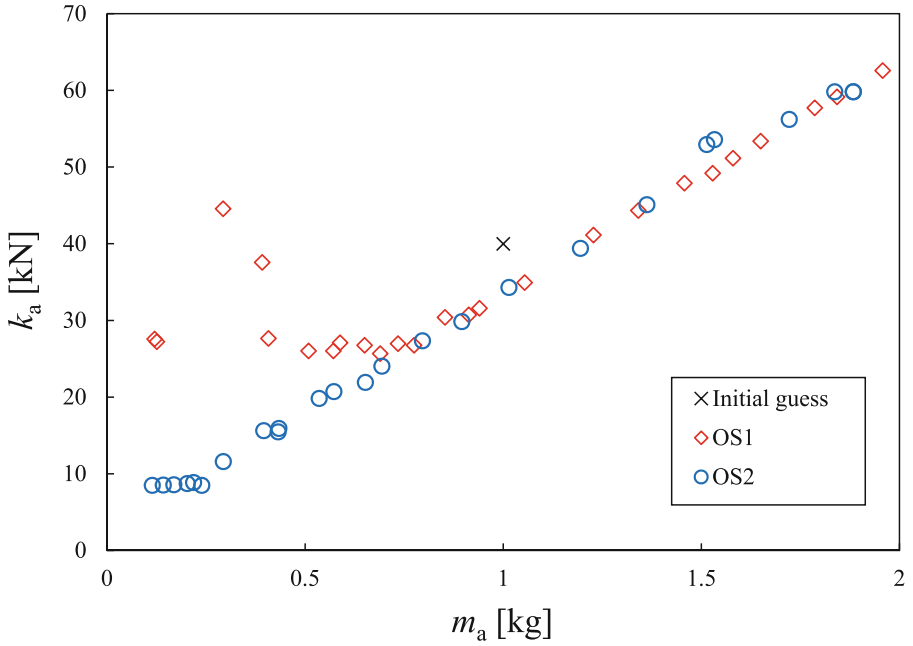

Fig. 4.8 Pareto sets for the linear TMD

According to the Pareto optimized results obtained for the linear TMD, the minimum auxiliary mass and stiffness required for which the vibration is reduced are $m_{\mathrm{a}} \approx 0.8$ kg and $k_{\mathrm{a}} \approx 30$ kN, respectively (see, Figs. 4.8 and 4.9). The interesting point is that both Pareto sets associated with OS1 and OS2 for the linear TMD follow almost the same linear trend given by Eq. (4.18).

$$k_{\mathrm{a}} \approx 30000 m_{\mathrm{a}} + 3600, \quad m_{\mathrm{a}} \geq 0.8 \text{ kg} \tag{4.18}$$

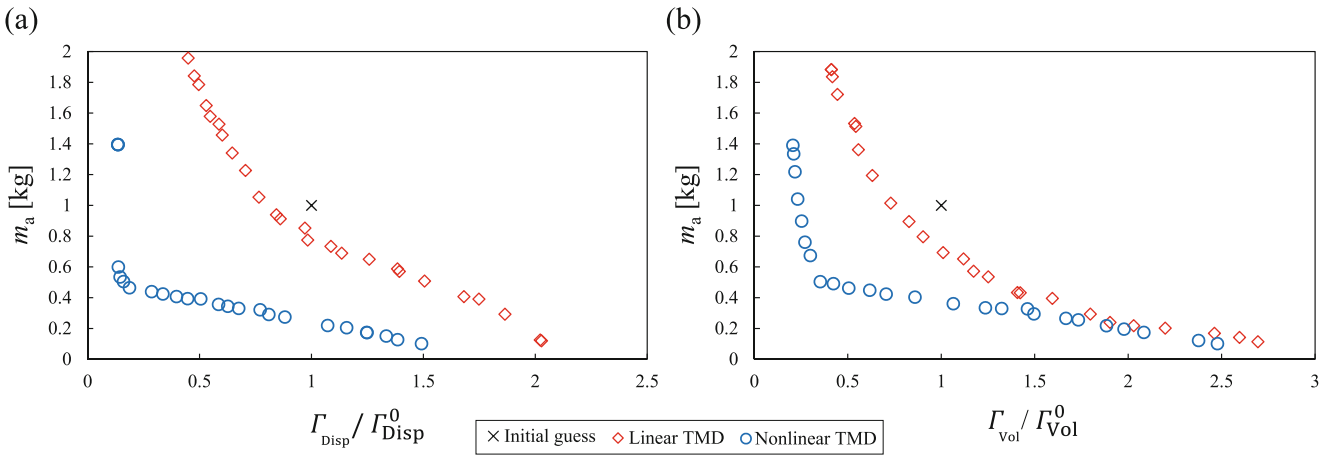

Fig. 4.9 Pareto fronts for the linear and nonlinear TMDs: (**a**) OS1; (**b**) OS2

Indeed, the Pareto sets achieved for OS1 and OS2 reveal that the optimization results are not affected by varying the reference exciting force amplitude ($F_{e_{ref}}$). This is in agreement with the GSA results shown in Fig. 4.4. Therefore, with the aid of the GSA, one can carry out the multiobjective optimization for a constant reference exciting force amplitude ($F_{e_{ref}}$) and expect that the obtained Pareto optimized results are valid for the case that the exciting force amplitude ($F_{e_{ref}}$) is also varies on the desired range. This can significantly reduce the computational efforts.

From the Pareto fronts shown in Fig. 4.9a, b it can be seen that the linear TMD can slightly reduce the vibrations in the HHIM. However, there are only few Pareto optimal points which simultaneously minimize both objective functions (i.e. lead to a lighter HHIM ($m_a < 1$) and lower vibrations in terms of Γ_{Disp} and Γ_{Vol} (i.e. $\Gamma_{Disp}/\Gamma^0_{Disp} < 1$ and $\Gamma_{Vol}/\Gamma^0_{Vol} < 1$).

In contrast, the Pareto fronts associated with the nonlinear TMD obtained for OS1 and OS2 not only reduce the vibrations more efficiently in comparison with to the linear TMD, but also give more possibilities for the Pareto optimal solutions which can simultaneously minimize the total weight and vibrations of the HHIM in terms of Γ_{Disp} and Γ_{Vol} (see, blue circles in Fig. 4.9).

The Pareto sets associated with the nonlinear TMD are shown in Fig. 4.10 for OS1 and OS2. It should be noted that the 25 Pareto set points are sorted in a descending order with respect to the auxiliary mass (m_a). Indeed, lower numbers denote a heavier HHIM but less vibrations and higher numbers correspond to a lighter machine but more vibrations. It should be noted that there is a mapping between the Pareto sets shown in Fig. 4.10 and the Pareto fronts shown in Fig. 4.9. As an example, the values of the design parameters m_a, k_a, a, and F_0 associated with number one in Fig. 4.10 denote the optimal characteristics of the nonlinear TMD minimizing vibrations of the HHIM (the point corresponding to $m_a = 1.4$ kg in Fig. 4.9).

Similar to the linear case, higher auxiliary mass (m_a) and stiffer auxiliary stiffness (k_a) lead to a better vibration absorber capacity in comparison with to the initial configuration. As long as the auxiliary mass (m_a) decreases the unpleasant vibration level increases. The minimum auxiliary mass required to reduce the vibrations with respect to the initial configuration is around $m_a \approx 0.4$ kg which is half of the value attained by the linear analysis.

It is interesting to note that to some extend the Pareto optimized solutions associated with $\mathbf{\Gamma_{OS1}}$ and $\mathbf{\Gamma_{OS2}}$ are following the same trend. In other words, the multiobjective optimization results are not noticeably affected by varying the reference force amplitude ($F_{e_{ref}}$). This is in agreement with the GSA results shown in Fig. 4.6 and the linear TMD analysis. Therefore, one can run the multiobjective optimization of the nonlinear TMD for the OS1 and expect to get the same Pareto optimized solutions for OS2. This can significantly reduce the computational burden of optimization. As an example, assume that the optimization with respect to $\mathbf{\Gamma_{OS2}}$ is carried out by varying the reference force amplitude ($F_{e_{ref}}$) at n_f different points. This means that the simulation time required to run optimization with respect to $\mathbf{\Gamma_{OS2}}$ are n_f times the simulations required to run the optimization with respect to $\mathbf{\Gamma_{OS1}}$ (which is accomplished for one single value of $F_{e_{ref}}$). Therefore, the computational efficiency of the optimization can be significantly improved (n_f times faster) by using the GSA results.

It is also interesting to note that the Pareto set characteristics which denote the case with minimum vibration level (Pareto set points number 1) represent the same optimal values of the design parameters for both operational scenarios OS1 and OS2.

The maximum RMS of displacements (x_1, x_2, and x_3) for a fixed reference force amplitude ($F_{e_{ref}} = 351$ N) at different exciting frequencies (f) are plotted in Figs. 4.11 (a-c) for the in service configuration and three optimal cases with minimum

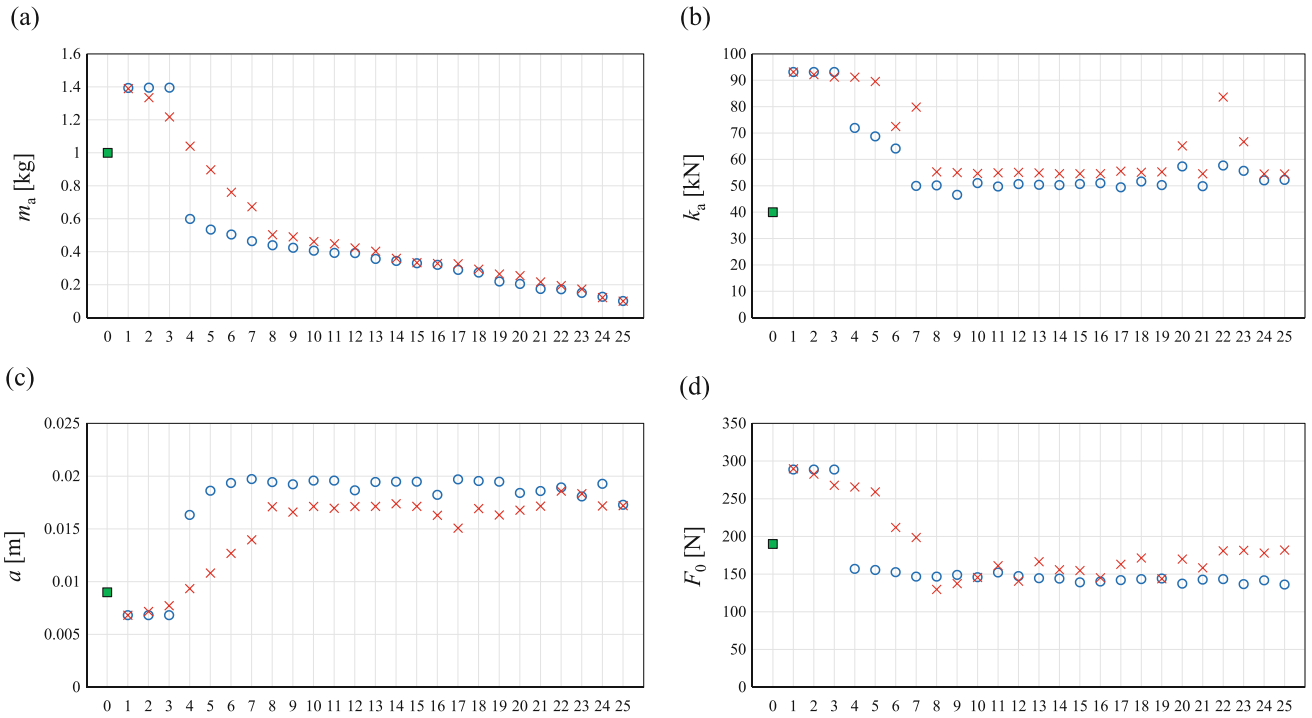

Fig. 4.10 Pareto sets for the nonlinear TMD: ■ initial guess; ∘ OS1; × OS2

and maximum auxiliary masses ($m_a = 0.1$ kg and $m_a = 1.4$ kg) as well as an interstitial mass ($m_a = 0.5$ kg). These optimal cases represent the point number 1, 25, and 5 from the Pareto set shown in Figs. 4.10 for OS1, respectively. It should be noted that the vertical axes in Figs. 4.11a-c are in logarithmic scale. From Fig. 4.11c it can be seen that by using the Pareto optimized values of the design parameters corresponding to $m_a = 1.4$ kg minimum vibration level can be achieved. However, the total mass of the HHIM will be increased by 0.4 kg. By choosing $m_a = 0.5$ kg, makes it possible to simultaneously reduce the weight of the HHIM (by 0.5 kg) and vibrations in x_3 (See Fig. 4.11c). The weight of the HHIM can be reduced by maximum 0.9 kg (using $m_a = 0.1$ kg). However, this would increase the vibration level. Similar behavior is observed for maximum RMS of x_1 shown in Fig. 4.11a. The maximum RMS of the displacement of the auxiliary mass (x_2) is also shown in Fig. 4.11b.

The system vibration response corresponding to the in service and optimized design parameters are compared in Fig. 4.12 for the case that both the exciting force frequency and amplitude are varying on the prescribed design range. Here, the set which gives minimum vibration (point number one for OS2 in the Pareto set shown in Fig. 4.10) is chosen as the optimized case. The vibrations of the HHIM (maximum RMS of x_3) are significantly mitigated by using the Pareto optimized values of the design parameters compared to the in service case. It should be noted that for exciting frequencies around 24 Hz and reference force amplitudes close to 400 N the vibrations of the HHIM (maximum RMS of x_3) are increased using the optimized values of the design parameters compared to the in service case. This shows one of the limitations of the passive TMD technology.

4.6.3 Closed-Form Representation

In this section the nonlinear least squares method is utilized to develop closed-form formulas that express the relation between the optimal values of TMD design parameters (auxiliary stiffness (k_a), gap (a), and preload (F_0)) as functions of the auxiliary mass (m_a). Indeed, it is assumed that the optimal values of the auxiliary stiffness (k_a), gap (a), and preload (F_0) are expressed as a function of the auxiliary mass (m_a) through the following functional relationship:

$$f_i(m_a) \approx \frac{\alpha}{\beta + \delta(m_a)^\gamma}, \quad f_i = k_a, a, F_0. \tag{4.19}$$

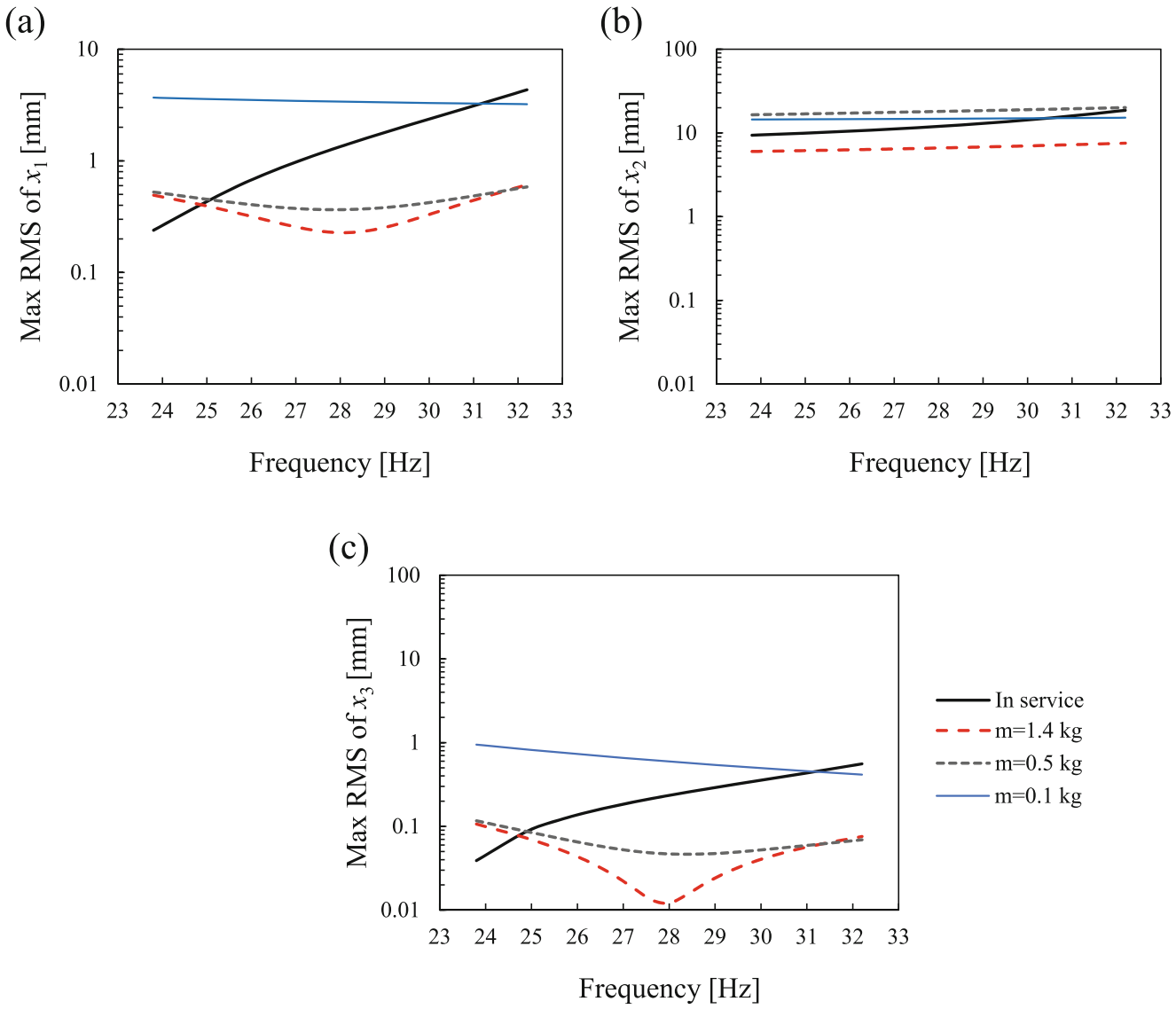

Fig. 4.11 The system vibration response with initial and some optimized cases

The variables α, β, δ, and γ have been determined by using the nonlinear least squares method based on the Pareto optimized solutions shown in Fig. 4.10, and given by Eq. (4.20):

$$k_{\mathrm{a}}\left(m_{\mathrm{a}}\right) \approx \frac{40e3}{0.368 + 0.087(m_{\mathrm{a}})^{-1.761}},$$

$$a\left(m_{\mathrm{a}}\right) \approx \frac{0.009}{0.452 + 0.444(m_{\mathrm{a}})^{2.258}},$$

$$F_0\left(m_{\mathrm{a}}\right) \approx \frac{190}{0.227 + 0.532(m_{\mathrm{a}})^{-0.853}}. \tag{4.20}$$

The closed-form formulas given by Eqs. (4.20) make it possible to approximate the optimal values of the design parameters of the TMD for given values of the auxiliary mass (0.4 kg $\leq m_{\mathrm{a}} \leq$ 1.4 kg). Functions $k_{\mathrm{a}}(m_{\mathrm{a}})$, $a(m_{\mathrm{a}})$, and $F_0(m_{\mathrm{a}})$ are plotted in Fig. 4.13a–c and compared with the respective values from Pareto set shown in Fig. 4.10. It can be seen that there exist an appropriate correlation between the Pareto set data and the fitted functions.

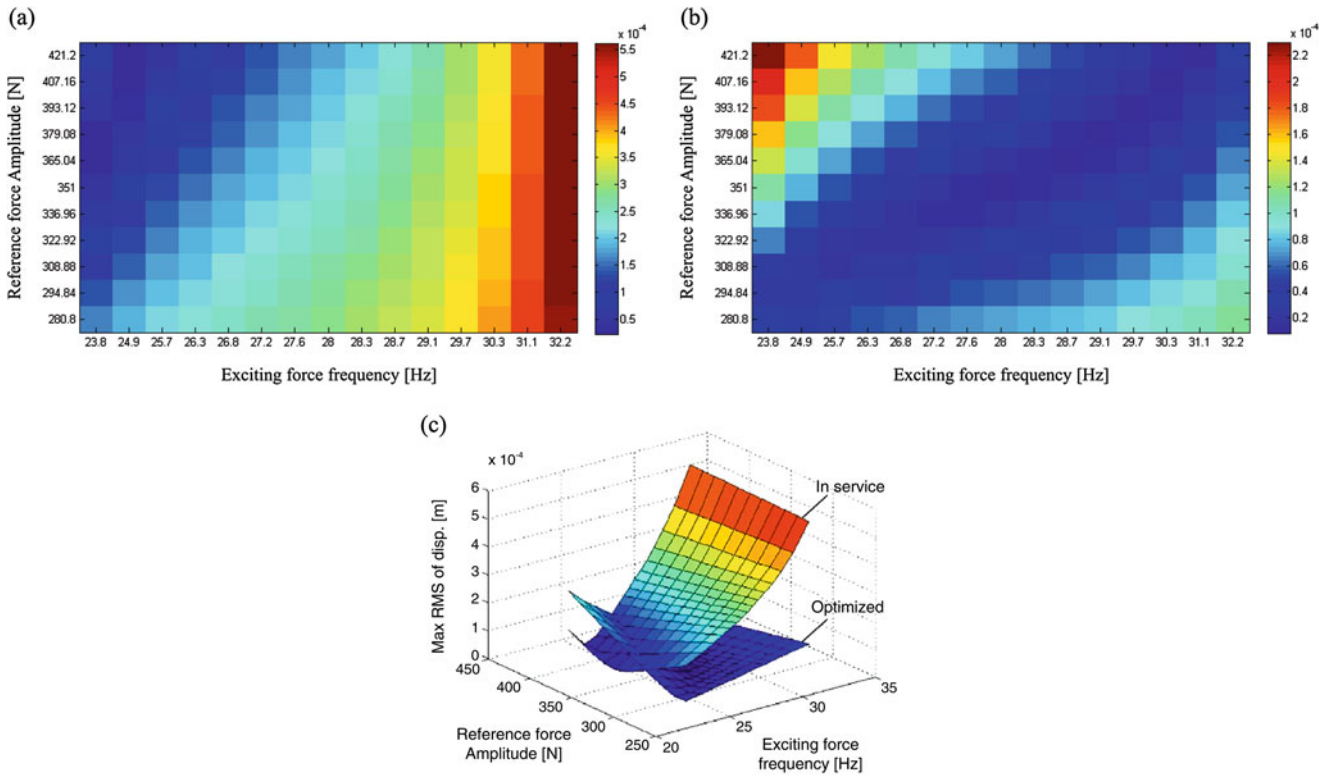

Fig. 4.12 The system vibration response: (**a**) In service; (**b**) optimized; (**c**) In service vs. optimized

In a similar manner, the nonlinear least squares method is utilized to develop a closed-form expression for the objective function Γ_{Vol} as a function of the auxiliary mass (m_{a}). It is given by Eq. (4.21).

$$f_{\Gamma_{\text{Vol}}}(m_a)/\Gamma^0_{\text{Vol}} = -3.209 - 1.855(m_{\text{a}})^{-0.149} + 0.987\left(\frac{k_{\text{a}}}{40e3}\right)^{1.692} + 1.269\left(\frac{a}{0.009}\right)^{1.393} + 0.32\left(\frac{F_0}{190}\right)^{-4.795}. \quad (4.21)$$

Here, $k_{\text{a}}(m_{\text{a}})$, $a(m_{\text{a}})$, and $F_0(m_{\text{a}})$ are evaluated using Eqs. (4.20).

The normalized function $f_{\Gamma_{\text{Vol}}}$ given by Eq. (4.21) is compared with simulation results and the Pareto front associated with OS2 (shown in Fig. 4.9b) in Fig. 4.14. The simulation results are achieved by varying the auxiliary mass at 13 equally distributed points in the range of 0.4 kg $\leq m_{\text{a}} \leq$ 1.4 kg. The corresponding values of the stiffness (k_{a}), gap (a), and preload (F_0) are then evaluated using Eqs. (4.20). For these values of the nonlinear TMD parameters the system vibration response is evaluated through direct simulation by using Eqs. (4.1, 4.2 and 4.3) and expressions (4.5 and 4.7) and is plotted in Fig. 4.14.

It can be seen that there is a good correlation between the Pareto front, fitted function (Eq. (4.21)), and simulation results. Therefore, for a desired value of the auxiliary mass (0.4 kg $\leq m_{\text{a}} \leq$ 1.4 kg), using Eqs. (4.20, 4.21) makes it possible to approximate the corresponding optimal values of the auxiliary stiffness (k_{a}), gap (a), preload (F_0) as well as the system response (Γ_{Vol}) for the considered 3 DOF system and prescribed structural parameters without running simulations.

4.7 Conclusion

GSA and multidisciplinary design optimization of a linear and a nonlinear TMD have been considered to reduce the total weight and vibrations in a 3 DOF system which represents a HHIM. The M-DRM has been employed to carry out the GSA in an efficient manner and reduce the number of input variables for optimization. GA has been utilized to perform the multiobjective optimization. Using the least squares method and Pareto optimization the analytical expressions for the stiffness, gap, and spring preload as functions of the auxiliary mass of the nonlinear TMD have been obtained.

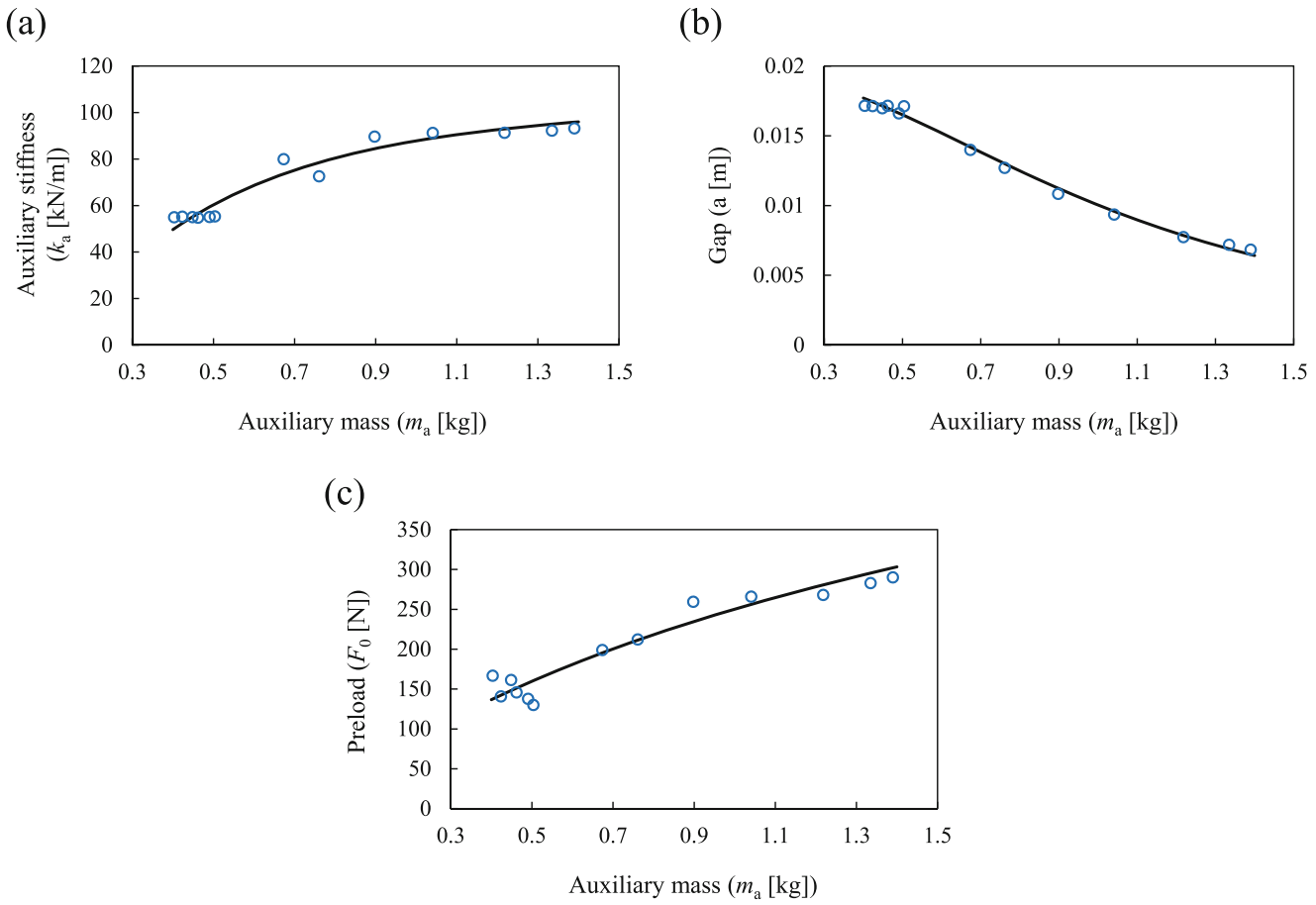

Fig. 4.13 Variation of optimal values of design parameters of the TMD with respect to auxiliary mass: (**a**) $k_a(m_a)$; (**b**) $a(m_a)$; (**c**) $F_0(m_a)$. Pareto optimized solutions (∘); fitted functions (—)

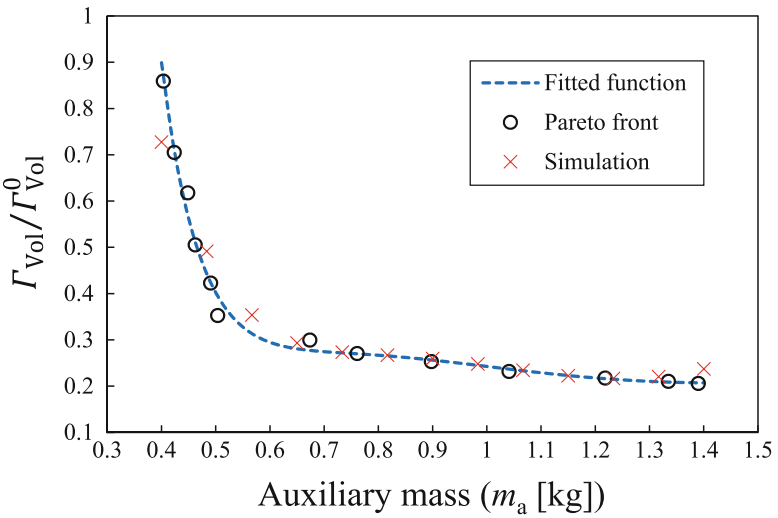

Fig. 4.14 Variation of $\boldsymbol{\Gamma_{Vol}/\Gamma^0_{Vol}}$ against the auxiliary mass (m_a)

Finally, the following concluding remarks have been drawn:

- Linear model of the TMD has limitations in design of the HHIM and a nonlinear TMD model should be considered in practice. Indeed, the nonlinear TMD has more vibration absorption capacity rather than a linear one.
- The optimization results for the case that only the frequency of the exciting force was varying were close to those associated with the case that both frequency and amplitude of the exciting force were varying.
- The GSA results showed that the exciting force amplitude does not influence the system response as much as the TMD parameters. Therefore, instead of running simulations with different exciting force frequency and amplitude, one can merely shift the exciting frequency and get optimization results that are robust against exciting force amplitude. This can significantly reduce the computational effort of optimization.
- The Pareto optimized solutions provided several design possibilities to reduce the harsh vibrations and/or the total weight of the system.

Although the Pareto optimized solutions give the possibility to operate the HHIM with lower harsh amplitudes, in certain ranges of frequency and exciting force amplitude, the optimized results might worsen the condition in comparison with to those corresponding to the HHIM with in-service structural data. This shows the limitation of the passive vibration control using TMD technology in application to HHIMs and further studies can be laid within robustness analysis of the optimization results achieved with respect to uncertainties in the design parameters. Active control of HHIMs can also be considered as an interesting focus for further analysis in this field.

Acknowledgments This work was financially supported by the Ekman family foundation and the Sweden's Innovation Agency (VINNOVA) through the project "Noll Vibrationsskador-steg 2" (Dnr: 2015-00352), which are gratefully acknowledged. The authors also would like to thank Hans Lindell and Snævar Leó Grétarsson, Swerea IVF AB, Mölndal, Sweden for interesting communication and fruitful discussions.

References

1. Yang, Y., Dai, W., Liu, Q.: Design and implementation of two-degree-of-freedom tuned mass damper in milling vibration mitigation. J. Sound Vib. **335**(2015), 78–88 (2015). https://doi.org/10.1016/j.jsv.2014.09.032
2. Li, S., Tang, J.: On vibration suppression and energy dissipation using tuned mass particle damper. J Vib Acoust. **139**(011008), 1–10 (2017). https://doi.org/10.1115/1.4034777
3. Dinh, V.-N., Basu, B.: Passive control of floating offshore wind turbine nacelle and spar vibrations by multiple tuned mass dampers. Struct. Control. Health Monit. **22**, 152–176 (2015). https://doi.org/10.1002/stc.1666
4. Mrabet, E., Guedri, M., Ichchou, M., Ghanmi, S.: New approaches in reliability based optimization of tuned mass damper in presence of uncertain bounded parameters. J. Sound Vib. **355**, 93–116 (2015). https://doi.org/10.1016/j.jsv.2015.06.009
5. Venanzi, I.: Robust optimal design of tuned mass dampers for tall buildings with uncertain parameters. Struct. Multidiscip. Optim. **51**, 239–250 (2015). https://doi.org/10.1007/s00158-014-1129-4
6. Lievens, K., Lombaert, G., Roeck, G.D., den Broeck, P.V.: Robust design of a TMD for the vibration serviceability of a footbridge. Eng. Struct. **123**, 408–418 (2016). https://doi.org/10.1016/j.engstruct.2016.05.028
7. Miguel, L.F.F., Lopez, R.H., Torii, A.J., Miguel, L.F.F., Beck, A.T.: Robust design optimization of TMDs in vehicle–bridge coupled vibration problems. Eng. Struct. **126**, 703–711 (2016). https://doi.org/10.1016/j.engstruct.2016.08.033
8. Tripathi, A., Grover, P., Kalmár-Nagy, T.: On optimal performance of nonlinear energy sinks in multiple-degree-of-freedom systems. J. Sound Vib. **388**, 272–297 (2017). https://doi.org/10.1016/j.jsv.2016.10.025
9. Marano, G.C., Quaranta, G., Greco, R.: Multi-objective optimization by genetic algorithm of structural systems subject to random vibrations. Struct. Multidiscip. Optim. **39**(4), 385–399 (2009). https://doi.org/10.1007/s00158-008-0330-8
10. Ribeiro, E.A., Pereira, J.T., Bavastri, C.A.: Passive vibration control in rotor dynamics: optimization of composed support using viscoelastic materials. J. Sound Vib. **351**, 43–56 (2015). https://doi.org/10.1016/j.jsv.2015.04.007
11. Mousavi Bideleh, S.M., Berbyuk, V., Persson, R.: Wear/comfort Pareto optimisation of bogie suspension. Veh. Syst. Dyn. **54**(8), 1053–1076 (2016). https://doi.org/10.1080/00423114.2016.1180405
12. Ok, S.-Y., Song, J., Park, K.-S.: Development of optimal design formula for bi-tuned mass dampers using multi-objective optimization. J. Sound Vib. **322**, 60–77 (2009). https://doi.org/10.1016/j.jsv.2008.11.023
13. Mohtat, A., Dehghan-Niri, E.: Generalized framework for robust design of tuned mass damper systems. J. Sound Vib. **330**, 902–922 (2011). https://doi.org/10.1016/j.jsv.2010.09.007
14. Greco, R., Marano, G.C., Fiore, A.: Performance–cost optimization of tuned mass damper under low-moderate seismic actions. Struct Des Tall Special Build. **25**, 1103–1122 (2016). https://doi.org/10.1002/tal.1300
15. Detroux, T., Habib, G., Masset, L., Kerschen, G.: Performance, robustness and sensitivity analysis of the nonlinear tuned vibration absorber. Mech. Syst. Signal Process. **60-61**, 799–809 (2015). https://doi.org/10.1016/j.ymssp.2015.01.035
16. Zhang, X., Pandey, M.D.: An effective approximation for variance-based global sensitivity analysis. Reliab. Eng. Syst. Saf. **121**, 164–174 (2014)
17. Mousavi Bideleh, S.M., Berbyuk, V.: Global sensitivity analysis of bogie dynamics with respect to suspension components. Multibody Sys Dyn. **37**(2), 145–174 (2016). https://doi.org/10.1007/s11044-015-9497-0

18. Mousavi-Bideleh, S.M., Berbyuk, V.: Multiobjective optimisation of bogie suspension to boost speed on curves. Veh. Syst. Dyn. **54**(1), 58–85 (2016). https://doi.org/10.1080/00423114.2015.1114655
19. Lindell, H., Berbyuk, V., Josefsson, M., and Grétarsson, S.L.: Nonlinear dynamic absorber to reduce vibration in hand-held impact machines. In International Conference on Engineering Vibration. Ljubljana, Slovenia, pp. 1530–1539 (2015)
20. Li, G., Rosenthal, C., Rabitz, H.: High dimensional model representations. Chem. A Eur. J. **105**, 7765–7777 (2001)
21. Sobol', I.M.: Global sensitivity indices for nonlinear mathematical models and their Monte Carlo estimates. Math. Comput. Simul. **55**, 271–280 (2001)
22. Sobol', I.M.: Theorems and examples on high dimensional model representation. Reliab. Eng. Syst. Saf. **79**, 187–193 (2003)
23. Mousavi Bideleh, S.M.: Robustness analysis of bogie suspension components Pareto optimized values. Veh. Syst. Dyn. **55**(8), 1189–1205 (2017). https://doi.org/10.1080/00423114.2017.1305115
24. Mousavi Bideleh, S.M., and Berbyuk, V.: Acomputer code for sensitivity analysis and multiobjective optimization: SAMO tutorial. Research report 2017:01, Chalmers University of Technology, Gothenurg, Sweden